Test of Lepton Universality Using $B^+ \to K^+\ell^+\ell^-$ Decays

R. Aaij *et al.*[*]
(LHCb Collaboration)

(Received 25 June 2014; published 6 October 2014)

A measurement of the ratio of the branching fractions of the $B^+ \to K^+\mu^+\mu^-$ and $B^+ \to K^+e^+e^-$ decays is presented using proton-proton collision data, corresponding to an integrated luminosity of 3.0 fb^{-1}, recorded with the LHCb experiment at center-of-mass energies of 7 and 8 TeV. The value of the ratio of branching fractions for the dilepton invariant mass squared range $1 < q^2 < 6$ GeV$^2/c^4$ is measured to be $0.745^{+0.090}_{-0.074}(\text{stat}) \pm 0.036(\text{syst})$. This value is the most precise measurement of the ratio of branching fractions to date and is compatible with the standard model prediction within 2.6 standard deviations.

DOI: 10.1103/PhysRevLett.113.151601 PACS numbers: 11.30.Hv

The decay $B^+ \to K^+\ell^+\ell^-$, where ℓ represents either a muon or an electron, is a $b \to s$ flavor-changing neutral current process. Such processes are highly suppressed in the standard model (SM) as they proceed through amplitudes involving electroweak loop (penguin and box) diagrams. This makes the branching fraction of $B^+ \to K^+\ell^+\ell^-$ (the inclusion of charge conjugate processes is implied throughout this Letter.) decays highly sensitive to the presence of virtual particles that are predicted to exist in extensions of the SM [1]. The decay rate of $B^+ \to K^+\mu^+\mu^-$ has been measured by LHCb to a precision of 5% [2] and, although the current theoretical uncertainties in the branching fraction are $\mathcal{O}(30\%)$ [3], these largely cancel in asymmetries or ratios of $B^+ \to K^+\ell^+\ell^-$ observables [2,4].

Owing to the equality of the electroweak couplings of electrons and muons in the SM, known as lepton universality, the ratio of the branching fractions of $B^+ \to K^+\mu^+\mu^-$ to $B^+ \to K^+e^+e^-$ decays [5] is predicted to be unity within an uncertainty of $\mathcal{O}(10^{-3})$ in the SM [1,6]. The ratio of the branching fractions is particularly sensitive to extensions of the SM that introduce new scalar or pseudoscalar interactions [1]. Models that contain a Z' boson have recently been proposed to explain measurements of the angular distribution and branching fractions of $B^0 \to K^{*0}\mu^+\mu^-$ and $B^+ \to K^+\mu^+\mu^-$ decays [7]. These types of models can also affect the relative branching fractions of $B^+ \to K^+\ell^+\ell^-$ decays if the Z' boson does not couple equally to electrons and muons.

Previous measurements of the ratio of branching fractions from e^+e^- colliders operating at the $\Upsilon(4S)$ resonance have measured values consistent with unity with a precision of 20%–50% [8]. This Letter presents the most precise measurement of the ratio of branching fractions and the corresponding branching fraction $\mathcal{B}$ $(B^+ \to K^+e^+e^-)$ to date. The data used for these measurements are recorded in proton-proton $(p\ p)$ collisions and correspond to 3.0 fb^{-1} of integrated luminosity, collected by the LHCb experiment at center-of-mass energies of 7 and 8 TeV.

The value of R_K within a given range of the dilepton mass squared from q^2_{min} to q^2_{max} is given by

$$R_K = \frac{\int_{q^2_{\text{min}}}^{q^2_{\text{max}}} \frac{d\Gamma[B^+ \to K^+\mu^+\mu^-]}{dq^2} dq^2}{\int_{q^2_{\text{min}}}^{q^2_{\text{max}}} \frac{d\Gamma[B^+ \to K^+e^+e^-]}{dq^2} dq^2}, \tag{1}$$

where Γ is the q^2 -dependent partial width of the decay. We report a measurement of R_K for $1 < q^2 < 6$ GeV$^2/c^4$. This range is both experimentally and theoretically attractive as it excludes the $B^+ \to J/\psi(\to \ell^+\ell^-)K^+$ resonant region, and precise theoretical predictions are possible. The high q^2 region, above the $\psi(2S)$ resonance, is affected by broad charmonium resonances that decay to lepton pairs [9].

The value of R_K is determined using the ratio of the relative branching fractions of the decays $B^+ \to K^+\ell^+\ell^-$ and $B^+ \to J/\psi(\to \ell^+\ell^-)K^+$, with $\ell = e$ and μ, respectively. This takes advantage of the large $B^+ \to J/\psi K^+$ branching fraction to cancel potential sources of systematic uncertainty between the $B^+ \to K^+\ell^+\ell^-$ and $B^+ \to J/\psi(\to \ell^+\ell^-)K^+$ decays as the efficiencies are correlated and the branching fraction to $B^+ \to J/\psi K^+$ is known precisely [10]. This is achieved by using the same selection for $B^+ \to K^+\ell^+\ell^-$ and $B^+ \to J/\psi(\to \ell^+\ell^-)K^+$ decays for each leptonic final state and by assuming lepton universality in the branching fractions of J/ψ mesons to the $\mu^+\mu^-$ and e^+e^- final states [10]. In terms of measured quantities, R_K is written as

$$R_K = \left(\frac{\mathcal{N}_{K^+\mu^+\mu^-}}{\mathcal{N}_{K^+e^+e^-}}\right)\left(\frac{\mathcal{N}_{J/\psi(e^+e^-)K^+}}{\mathcal{N}_{J/\psi(\mu^+\mu^-)K^+}}\right) \times \left(\frac{\epsilon_{K^+e^+e^-}}{\epsilon_{K^+\mu^+\mu^-}}\right)\left(\frac{\epsilon_{J/\psi(\mu^+\mu^-)K^+}}{\epsilon_{J/\psi(e^+e^-)K^+}}\right), \tag{2}$$

[*] Full author list given at the end of the article.

where $\mathcal{N}_X$ is the observed yield in final state X, and ϵ_X is the efficiency to trigger, reconstruct, and select that final state. Throughout this Letter the number of $K^+\mu^+\mu^-$ and $K^+e^+e^-$ candidates always refers to the restricted q^2 range, $1 < q^2 < 6\ \mathrm{GeV}^2/c^4$.

The LHCb detector is a single-arm forward spectrometer covering the pseudorapidity range $2 < \eta < 5$ and is described in detail in Ref. [11]. The simulated events used in this analysis are produced using the software described in Refs. [12].

Candidate $B^+ \to K^+\ell^+\ell^-$ events are first required to pass the hardware trigger that selects either muons with a high transverse momentum (p_T) or large energy deposits in the electromagnetic or hadronic calorimeters, which are a signature of high-p_T electrons or hadrons. Events with muons in the final state are required to be triggered by one or both muons in the hardware trigger. Events with electrons in the final state are required to be triggered by either one of the electrons, the kaon from the B^+ decay, or by other particles in the event. In the subsequent software trigger, at least one of the final-state particles is required to both have $p_T > 800\ \mathrm{MeV}/c$ and not to originate from any of the primary pp interaction vertices (PVs) in the event. Finally, the tracks of the final-state particles are required to form a vertex that is significantly displaced from the PVs. A multivariate algorithm [13] is used for the identification of secondary vertices consistent with the decay of a b hadron.

A $K^+\ell^+\ell^-$ candidate is formed from a pair of well-reconstructed oppositely charged particles identified as either electrons or muons, combined with another track that is identified as a charged kaon. Each particle is required to have $p_T > 800\ \mathrm{MeV}/c$ and be inconsistent with coming from any PV. The two leptons are required to originate from a common vertex, which is significantly displaced from all of the PVs in the event. The $K^+\ell^+\ell^-$ candidate is required to have a good vertex fit, and the $K^+\ell^+\ell^-$ candidate is required to point to the best PV, defined by the lowest impact parameter (IP).

Muons are initially identified by tracks that penetrate the calorimeters and the iron filters in the muon stations [14]. Further muon identification is performed with a multivariate classifier that uses information from the tracking system, the muon chambers, the ring-imaging Cherenkov (RICH) detectors and the calorimeters to provide separation of muons from pions and kaons. Electron identification is provided by matching tracks to an electromagnetic calorimeter (ECAL) cluster, combined with information from the RICH detectors, to build an overall likelihood for separating electrons from pions and kaons.

Bremsstrahlung from the electrons can significantly affect the measured electron momentum and the reconstructed B^+ candidate mass. To improve the accuracy of the electron momentum reconstruction, a correction for the measured momenta of photons associated to the electron is applied. If an electron radiates a photon downstream of the dipole magnet, the photon enters the same ECAL cells as the electron itself and the original energy of the electron is measured by the ECAL. However, if an electron radiates a photon upstream of the dipole magnet, the energy of the photon will not be deposited in the same ECAL cells as the electron. After correction, the ratio of electron energy to the momentum measured by the ECAL is expected to be consistent with unity; the ratio is used in the electron identification likelihood. Since there is little material within the magnet for particle interactions to cause additional neutral particles, the ECAL cells without an associated track are used to look for bremsstrahlung photons. A search is made for photons with transverse energy greater than 75 MeV within a region of the ECAL defined by the extrapolation of the electron track upstream of the magnet.

The separation of the signal from combinatorial background uses a multivariate algorithm based on boosted decision trees (BDT) [15]. Independent BDTs are trained to separate the dielectron and dimuon signal decays from combinatorial backgrounds. The BDTs are trained using $B^+ \to J/\psi(\to \mu^+\mu^-)K^+$ and $B^+ \to J/\psi(\to e^+e^-)K^+$ candidates in data to represent the signal, and candidates with $K^+\ell^+\ell^-$ masses $m(K^+\ell^+\ell^-) > 5700\ \mathrm{MeV}/c^2$ as the background sample. The latter sample is not used in the subsequent analysis. The variables used as input to the BDTs are the transverse momentum of the B^+ candidate and of the final state particles, the B^+ decay time, the vertex fit quality, the IP of the B^+ candidate, the angle between the B^+ candidate momentum vector and direction between the best PV and the decay vertex, the IP of the final-state particles to the best PV and the track fit quality. The most discriminating variable is the vertex quality for the B^+ and the angle between the B^+ candidate and the best PV. The selections are optimized for the significance of the signal yield for each $B^+ \to K^+\ell^+\ell^-$ decay and accept 60%–70% of the signal, depending on the decay channel, while rejecting over 95% of the combinatorial background. The efficiency of the BDT response is uniform across the q^2 region of interest and in the J/ψ region, ensuring that the selection is not significantly biased by the use of the $B^+ \to J/\psi(\to \ell^+\ell^-)K^+$ data.

After applying the selection criteria, exclusive backgrounds from b -hadron decays are dominated by three sources. The first is misreconstructed $B^+ \to J/\psi(\to \ell^+\ell^-)K^+$ and $B^+ \to \psi(2S)(\to \ell^+\ell^-)K^+$ decays where the kaon is mistakenly identified as a lepton and the lepton (of the same electric charge) as a kaon. Such events are excluded using different criteria for the muon and the electron modes owing to the lower momentum resolution in the latter case. The $B^+ \to K^+\mu^+\mu^-$ candidates are kept if the kaon passes through the acceptance of the muon detectors and is not identified as a muon, or if the mass of the kaon candidate (in the muon mass hypothesis) and

the oppositely charged muon candidate pair is distinct from the J/ψ or the $\psi(2S)$ resonances. The $B^+ \to K^+e^+e^-$ candidates are kept if the kaon has a low probability of being an electron according to the information from the electromagnetic and hadronic calorimeters and the RICH system. The second source of background is from semileptonic decays such as $B^+ \to \bar{D}^0(\to K^+\pi^-)\ell^+\nu_\ell$, or $B^+ \to \bar{D}^0\pi^+$, with $\bar{D}^0 \to K^+\ell^-\bar{\nu}_\ell$ or $\pi^+\ell^-\bar{\nu}_\ell$, which can be selected as signal decays if at least one of the hadrons is mistakenly identified as a lepton. All of these decays are vetoed by requiring that the mass of the $K^+\ell^-$ pair, where the lepton is assigned the pion mass, is greater than 1885 MeV/c^2. These vetoes result in a negligible loss of signal as measured in simulation. The third source of background is partially reconstructed b -hadron decays that are reconstructed with masses smaller than the measured B^+ mass. In the muon decay modes, this background is excluded by the choice of $m(K^+\mu^+\mu^-)$ mass interval, while in the electron modes this background is described in the mass fit model. Fully hadronic b -meson decays, such as $B^+ \to K^+\pi^+\pi^-$, are reduced to $\mathcal{O}(0.1\%)$ of the $B^+ \to K^+\mu^+\mu^-$ and $B^+ \to K^+e^+e^-$ signals by the electron and muon identification requirements, respectively, and are neglected in the analysis.

The reconstructed B^+ mass and dilepton mass of the candidates passing the selection criteria are shown in Fig. 1. It is possible to see the pronounced peaks of the J/ψ and $\psi(2S)$ decays along with their radiative tail as a diagonal band. Partially reconstructed decays can be seen to lower $K^+\ell^+\ell^-$ masses and the distribution of random combinatorial background at high $K^+\ell^+\ell^-$ masses. Only candidates with $5175 < m(K^+\mu^+\mu^-) < 5700\,\text{MeV}/c^2$ or $4880 < m(K^+e^+e^-) < 5700$ MeV/c^2 are considered. The dilepton mass squared is also restricted to $1 < q^2 < 6$ GeV$^2/c^4$, $8.68 < q^2 < 10.09$ GeV$^2/c^4$ and $6 < q^2 < 10.09\,\text{GeV}^2/c^4$ when selecting $B^+ \to K^+\ell^+\ell^-$, $B^+ \to J/\psi(\to \mu^+\mu^-)K^+$ and $B^+ \to J/\psi(\to e^+e^-)K^+$ candidates, respectively.

The event yields for the $B^+ \to K^+\ell^+\ell^-$ and the $B^+ \to J/\psi(\to \ell^+\ell^-)K^+$ modes are determined using unbinned extended maximum likelihood fits to the $K^+\ell^+\ell^-$ mass distributions. The model is composed of a signal shape, a combinatorial background shape and, for the electron modes, a contribution from partially reconstructed b -hadron decays.

The signal mass model for the muon modes consists of the sum of two Crystal Ball functions [16] with tails above and below the mass peak. This empirical function describes the core of the mass distribution and additional effects from the experimental resolution and the radiative tail. The mean, width, and radiative tail parameters for the signal model are obtained from a fit to the $B^+ \to J/\psi(\to \mu^+\mu^-)K^+$ sample and propagated to the fit for the $B^+ \to K^+\mu^+\mu^-$ decays. The validity of this approach is verified using simulation. The combinatorial background is described by an exponential function. There are 667046 ± 882 $B^+ \to J/\psi(\to \mu^+\mu^-)K^+$ and 1226 ± 41 $B^+ \to K^+\mu^+\mu^-$ signal decays, where the uncertainties are statistical.

The mass distribution of the electron modes depends strongly on the number of bremsstrahlung photons that are associated with the electrons, and therefore a more involved parametrization is required. The mass distribution also depends on the p_T of the electrons and on the occupancy of the event. This shape dependence is studied using a selection of $B^+ \to J/\psi(\to e^+e^-)K^+$ events in the data. The data are split into three independent samples according to which particle in the event has fired the hardware trigger; a similar strategy was applied in Ref. [17]. These categories are mutually exclusive and consist of events selected either by one of the two electrons, by the K^+ meson, or by other particles. Events that are triggered by one of the electrons in the hardware trigger typically have larger electron

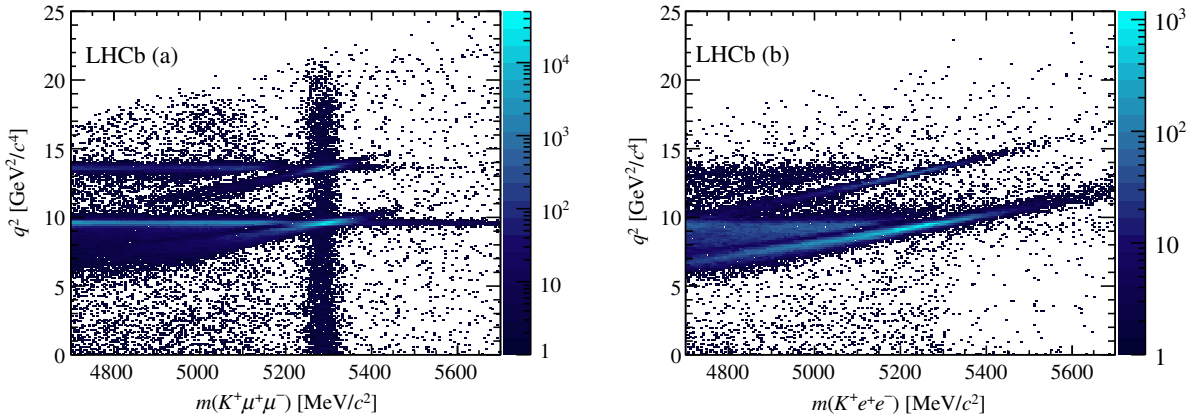

FIG. 1 (color online). Dilepton invariant mass squared q^2 as a function of the $K^+\ell^+\ell^-$ invariant mass, $m(K^+\ell^+\ell^-)$, for selected (a) $B^+ \to K^+\mu^+\mu^-$ and (b) $B^+ \to K^+e^+e^-$ candidates. The radiative tail of the J/ψ and $\psi(2S)$ mesons is most pronounced in the electron mode due to the larger bremsstrahlung and because the energy resolution of the ECAL is lower compared to the momentum resolution of the tracking system.

momentum and p_T than events triggered by the K^+ meson or other particles in the event. Within each of these trigger categories, independent shapes are used depending on the number of neutral clusters that are added to the dielectron candidate to correct for the effects of bremsstrahlung: one for candidates where no clusters are added to either electron; one for candidates where a cluster is added to one of the electrons; and one for candidates where clusters are added to both electrons. The fractions of candidates in each of these categories are 37%, 48%, and 15%, respectively, for both $B^+ \to J/\psi(\to e^+e^-)K^+$ and $B^+ \to K^+e^+e^-$ candidates. The relative proportion of the three categories for the number of additional clusters is described well by the simulation. Candidates with no added clusters have a large radiative tail to smaller $m(K^+e^+e^-)$ values. Candidates with one or more added clusters have a reduced radiative tail, but have larger tails above the expected B^+ mass due to the event occupancy or the resolution of the ECAL.

The parametrization of the $B^+ \to K^+e^+e^-$ mass distribution in each of the three trigger categories is described by a sum of three Crystal Ball functions, each of which has independent values for the peak, width, and radiative tail, representing the different number of clusters that are added. The parameters for each of the Crystal Ball functions are found by fitting the $m(K^+e^+e^-)$ distribution of the $B^+ \to J/\psi(\to e^+e^-)K^+$ candidates. A high-purity sample of $B^+ \to J/\psi(\to e^+e^-)K^+$ candidates is achieved by constraining the mass of the e^+e^- pair to the known J/ψ mass. A requirement that $m(J/\psi K^+)$ is greater than 5175 MeV/c^2 removes partially reconstructed signal candidates, leaving a prominent signal peak with negligible contribution from combinatorial backgrounds without biasing the mass shape.

The mass distribution of the partially reconstructed backgrounds is determined using simulated $H_b \to J/\psi(\to e^+e^-)X$ decays that satisfy the selection criteria, where H_b is a B^+, B^0, B_s^0, or Λ_b^0 hadron. The relative branching fraction of $H_b \to J/\psi(\to e^+e^-)X$ to $H_b \to e^+e^-X$ decays is assumed to be the same as that of $B^+ \to J/\psi(\to e^+e^-)K^+$ and $B^+ \to K^+e^+e^-$ decays, and is consistent with the observed ratios of $B^+ \to J/\psi(\to \mu^+\mu^-)K^+$ to $B^+ \to K^+\mu^+\mu^-$ decays and $B^0 \to J/\psi(\to \mu^+\mu^-)K^{*0}$ to $B^0 \to K^{*0}\mu^+\mu^-$ decays [10].

The ratio of partially reconstructed background to signal for the decay $B^+ \to K^+e^+e^-$ is determined by the ratio measured in $B^+ \to J/\psi(\to e^+e^-)K^+$ data for each trigger category, after correcting for two factors. First, the partially reconstructed backgrounds for the $B^+ \to J/\psi K^+$ data may include a contribution from cascade decays of higher $c\bar{c}$ resonances, e.g., $B^+ \to \psi(2S)(\to J/\psi\pi^+\pi^-)K^+$ or $B^+ \to \chi_c(\to J/\psi\gamma)K^+$ decays. These decays contribute to the $B^+ \to J/\psi K^+$ background but not to the partially reconstructed backgrounds for the $B^+ \to K^+e^+e^-$ data. The level of contamination is estimated using simulated inclusive $H_b \to J/\psi(\to e^+e^-)X$ decays and found to be $(16 \pm 1)\%$. Second, the dominant contribution to the $B^+ \to K^+e^+e^-$ background is from partially reconstructed $B^0 \to K^{*0}e^+e^-$ decays. The relative proportion of $B^0 \to K^{*0}\mu^+\mu^-$ to $B^+ \to K^+\mu^+\mu^-$ decays is known to be 10% higher than the relative proportion of $B^0 \to J/\psi K^{*0}$ to $B^+ \to J/\psi K^+$ decays [10]. The fraction of partially reconstructed background to signal is adjusted accordingly. The partially reconstructed backgrounds account for 16%–20% of the signal yields depending on the trigger category.

The results of the fits for the $B^+ \to J/\psi(\to e^+e^-)K^+$ and $B^+ \to K^+e^+e^-$ channels are shown in Fig. 2. In total there are 172^{+20}_{-19} (62324 ± 318) $B^+ \to K^+e^+e^-$ $(B^+ \to J/\psi(\to e^+e^-)K^+)$ decays triggered by the electron trigger, 20^{+16}_{-14} (9337 ± 124) decays triggered by the hadron trigger, and 62 ± 13 $(16\,796 \pm 165)$ decays that were triggered by other particles in the event.

It is possible for $B^+ \to K^+e^+e^-$ decays that emit bremsstrahlung to migrate out of the $1 < q^2 < 6$ GeV$^2/c^4$ range at the lower edge and in from the upper edge. The effect of this bin migration on the yield is determined using $B^+ \to K^+e^+e^-$ simulation and validated with $B^+ \to J/\psi(\to e^+e^-)K^+$ data. The corresponding uncertainty due to the dependence of the branching fraction on non-SM contributions is estimated by independantly varying the $B^+ \to K^+$ form factors and by adjusting the Wilson coefficients [18]. The overall yield of $B^+ \to K^+e^+e^-$ is scaled by $(90.9 \pm 1.5)\%$ to account for this migration, where the uncertainty is mainly due to the model dependence. The quality of the fits to the mass distribution of $K^+\ell^+\ell^-$ candidates is investigated and found to be acceptable.

The systematic dependence of the signal yield on the signal model is considered negligible for the muon modes due to the excellent dimuon mass resolution at LHCb [19]. The proportion of the partially reconstructed backgrounds is changed based on the measurements of the $B^+ \to (J/\psi \to e^+e^-)K^+X$ contribution in Refs. [20,21] and contributes a systematic uncertainty of 1.6% to the value of R_K. The uncertainty in the signal model for the $B^+ \to K^+e^+e^-$ mass distribution is assessed by incorporating a resolution effect that takes into account the difference between the mass shape in simulated events for $B^+ \to J/\psi(\to e^+e^-)K^+$ and $B^+ \to K^+e^+e^-$ decays and contributes a relative systematic uncertainty of 3% to the value of R_K.

The efficiency to select $B^+ \to K^+\mu^+\mu^-$, $B^+ \to K^+e^+e^-$, $B^+ \to J/\psi(\to \mu^+\mu^-)K^+$, and $B^+ \to J/\psi(\to e^+e^-)K^+$ decays is the product of the efficiency to reconstruct the final state particles. This includes the geometric acceptance of the detector, the trigger, and the selection efficiencies. Each of these efficiencies is determined from simulation and is corrected for known differences relative to data. The use of the double ratio of decay modes ensures that most of the possible sources of systematic uncertainty cancel when determining R_K. Residual effects from the trigger and the particle identification that do not cancel in the ratio arise

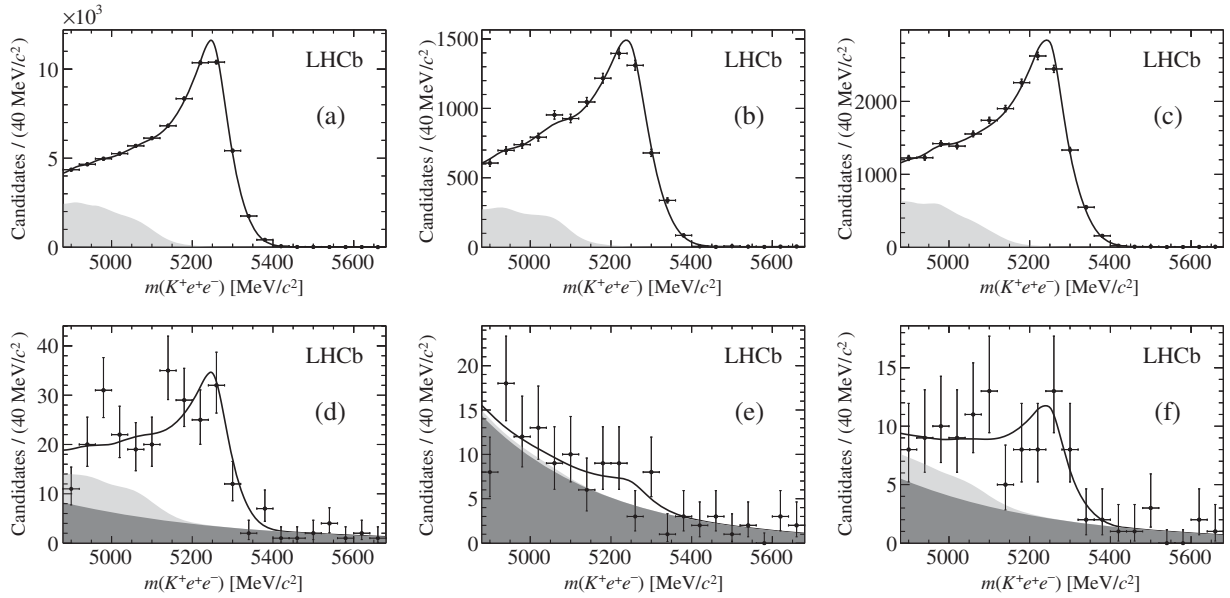

FIG. 2. Mass distributions with fit projections overlaid of selected $B^+ \to J/\psi(\to e^+e^-)K^+$ candidates triggered in the hardware trigger by (a) one of the two electrons, (b) by the K^+, and (c) by other particles in the event. Mass distributions with fit projections overlaid of selected $B^+ \to K^+e^+e^-$ candidates in the same categories, triggered by (d) one of the two electrons, (e) the K^+, and (f) by other particles in the event. The total fit model is shown in black, the combinatorial background component is indicated by the dark shaded region and the background from partially reconstructed b -hadron decays by the light shaded region.

due to different final-state particle kinematic distributions in the resonant and nonresonant dilepton mass region.

The dependence of the particle identification on the kinematic distributions contributes a systematic uncertainty of 0.2% to the value of R_K. The efficiency associated with the hardware trigger on $B^+ \to J/\psi(\to e^+e^-)K^+$ and $B^+ \to K^+e^+e^-$ decays depends strongly on the kinematic properties of the final state particles and does not entirely cancel in the calculation of R_K, due to different electron and muon trigger thresholds. The efficiency associated with the hardware trigger is determined using simulation and is cross-checked using $B^+ \to J/\psi(\to e^+e^-)K^+$ and $B^+ \to J/\psi(\to \mu^+\mu^-)K^+$ candidates in the data, by comparing candidates triggered by the kaon or leptons in the hardware trigger to candidates triggered by other particles in the event. The largest difference between data and simulation in the ratio of trigger efficiencies between the $B^+ \to K^+\ell^+\ell^-$ and $B^+ \to J/\psi(\to \ell^+\ell^-)K^+$ decays is at the level of 3%, which is assigned as a systematic uncertainty on R_K. The veto to remove misidentification of kaons as electrons contains a similar dependence on the chosen binning scheme and a systematic uncertainty of 0.6% on R_K is assigned to account for this.

Overall, the efficiency to reconstruct, select, and identify an electron is around 50% lower than the efficiency for a muon. The total efficiency in the range $1 < q^2 < 6\ \mathrm{GeV}^2/c^4$ is also lower for $B^+ \to K^+\ell^+\ell^-$ decays than the efficiency for the $B^+ \to J/\psi(\to \ell^+\ell^-)K^+$ decays, due to the softer lepton momenta in this q^2 range.

The ratio of efficiency-corrected yields of $B^+ \to K^+e^+e^-$ to $B^+ \to J/\psi(\to e^+e^-)K^+$ is determined separately for each type of hardware trigger and then combined with the ratio of efficiency-corrected yields for the muon decays. R_K is measured to have a value of $0.72^{+0.09}_{-0.08}(\mathrm{stat}) \pm 0.04(\mathrm{syst})$, $1.84^{+1.15}_{-0.82}(\mathrm{stat}) \pm 0.04(\mathrm{syst})$, and $0.61^{+0.17}_{-0.07}(\mathrm{stat}) \pm 0.04(\mathrm{syst})$ for dielectron events triggered by electrons, the kaon, or other particles in the event, respectively. Sources of systematic uncertainty are assumed to be uncorrelated and are added in quadrature. Combining these three independent measurements of R_K and taking into account correlated uncertainties from the muon yields and efficiencies, gives

$$R_K = 0.745^{+0.090}_{-0.074}(\mathrm{stat}) \pm 0.036(\mathrm{syst}).$$

The dominant sources of systematic uncertainty are due to the parametrization of the $B^+ \to J/\psi(\to e^+e^-)K^+$ mass distribution and the estimate of the trigger efficiencies that both contribute 3% to the value of R_K.

The branching fraction of $B^+ \to K^+e^+e^-$ is determined in the region from $1 < q^2 < 6\ \mathrm{GeV}^2/c^4$ by taking the ratio of the branching fraction from $B^+ \to K^+e^+e^-$ and $B^+ \to J/\psi(\to e^+e^-)K^+$ decays and multiplying it by the measured value of $\mathcal{B}(B^+ \to J/\psi K^+)$ and $J/\psi \to e^+e^-$ [10]. The value obtained is $\mathcal{B}(B^+ \to K^+e^+e^-) = [1.56^{+0.19}_{-0.15}(\mathrm{stat})\,^{+0.06}_{-0.04}(\mathrm{syst})] \times 10^{-7}$. This is the most precise measurement to date and is consistent with the SM expectation.

In summary, the ratio of branching fractions for $B^+ \to K^+\mu^+\mu^-$ and $B^+ \to K^+e^+e^-$ decays, R_K, is measured in the dilepton invariant mass squared range from $1 < q^2 < 6\ \mathrm{GeV}^2/c^4$ with a total precision of 10%. A new measurement of the differential branching fraction of $B^+ \to K^+e^+e^-$ is also reported. The value of R_K is the most precise measurement of this quantity to date. It is compatible with the SM expectation of close to unity to within 2.6 standard deviations calculated using the ratio of the likelihoods between the central value and the SM prediction.

We express our gratitude to our colleagues in the CERN accelerator departments for the excellent performance of the LHC. We thank the technical and administrative staff at the LHCb institutes. We acknowledge support from CERN and from the national agencies: CAPES, CNPq, FAPERJ, and FINEP (Brazil); NSFC (China); CNRS/IN2P3 (France); BMBF, DFG, HGF, and MPG (Germany); SFI (Ireland); INFN (Italy); FOM and NWO (Netherlands); MNiSW and NCN (Poland); MEN/IFA (Romania); MinES and FANO (Russia); MinECo (Spain); SNSF and SER (Switzerland); NASU (Ukraine); STFC (United Kingdom); NSF (USA). The Tier1 computing centers are supported by IN2P3 (France), KIT and BMBF (Germany), INFN (Italy), NWO and SURF (Netherlands), PIC (Spain), GridPP (United Kingdom). We are indebted to the communities behind the multiple open source software packages on which we depend. We are also thankful for the computing resources and the access to software R&D tools provided by Yandex LLC (Russia). Individual groups or members have received support from EPLANET, Marie Skłodowska-Curie Actions and ERC (European Union), Conseil général de Haute-Savoie, Labex ENIGMASS and OCEVU, Région Auvergne (France), RFBR (Russia), XuntaGal and GENCAT (Spain), Royal Society, and Royal Commission for the Exhibition of 1851 (United Kingdom).

[1] C. Bobeth, G. Hiller, and G. Piranishvili, J. High Energy Phys. 12 (2007) 040.
[2] R. Aaij *et al.* (LHCb Collaboration), J. High Energy Phys. 02 (2013) 105.
[3] C. Bobeth, G. Hiller, D. van Dyk, and C. Wacker, J. High Energy Phys. 01 (2012) 107; A. Khodjamirian, T. Mannel, and Y. Wang, J. High Energy Phys. 02 (2013) 010.
[4] R. Aaij *et al.* (LHCb Collaboration), Phys. Rev. Lett. **111**, 151801 (2013); R. Aaij *et al.* (LHCb Collaboration), J. High Energy Phys. 07 (2012) 133.
[5] G. Hiller and F. Krüger, Phys. Rev. D **69**, 074020 (2004).
[6] C. Bouchard, G. P. Lepage, C. Monahan, H. Na, and J. Shigemitsu, Phys. Rev. Lett. **111**, 162002 (2013).
[7] S. Descotes-Genon, J. Matias, and J. Virto, Phys. Rev. D **88**, 074002 (2013); R. Gauld, F. Goertz, and U. Haisch, J. High Energy Phys. 01 (2014) 069; A. J. Buras, F. De Fazio, J. Girrbach, and M. V. Carlucci, J. High Energy Phys. 02 (2013) 023; W. Altmannshofer and D. M. Straub, Eur. Phys. J. C **73**, 2646 (2013).
[8] J. P. Lees *et al.* (BaBar Collaboration), Phys. Rev. D **86**, 032012 (2012); J.-T. Wei *et al.* (Belle Collaboration), Phys. Rev. Lett. **103**, 171801 (2009).
[9] R. Aaij *et al.* (LHCb Collaboration), Phys. Rev. Lett. **111**, 112003 (2013).
[10] J. Beringer *et al.* (Particle Data Group), Phys. Rev. D **86**, 010001 (2012), and the 2013 partial update for the 2014 edition.
[11] A. A. Alves, Jr. *et al.* (LHCb Collaboration), JINST **3**, S08005 (2008).
[12] T. Sjöstrand, S. Mrenna, and P. Skands, Comput. Phys. Commun. **178**, 852 (2008); I. Belyaev *et al.*, in *Nuclear Science Symposium Conference Record (NSS/MIC), Knoxville, 2010* (IEEE, New York, 2010), p. 1155; D. J. Lange, Nucl. Instrum. Methods Phys. Res., Sect. A **462**, 152 (2001); P. Golonka and Z. Was, Eur. Phys. J. C **45**, 97 (2006); J. Allison *et al.* (Geant4 Collaboration), IEEE Trans. Nucl. Sci. **53**, 270 (2006); S. Agostinelli *et al.* (Geant4 Collaboration), Nucl. Instrum. Methods Phys. Res., Sect. A **506**, 250 (2003); M. Clemencic, G. Corti, S. Easo, C. R. Jones, S. Miglioranzi, M. Pappagallo, and P. Robbe, J. Phys. Conf. Ser. **331**, 032023 (2011).
[13] V. V. Gligorov and M. Williams, JINST **8**, P02013 (2013).
[14] F. Archilli *et al.*, JINST **8**, P10020 (2013).
[15] L. Breiman, J. H. Friedman, R. A. Olshen, and C. J. Stone, *Classification and Regression Trees* (Wadsworth Int. Group, Belmont, CA, 1984); B. P. Roe, H.-J. Yang, J. Zhu, Y. Liu, I. Stancu, and G. McGregor, Nucl. Instrum. Methods Phys. Res., Sect. A **543**, 577 (2005).
[16] T. Skwarnicki, Ph.D. thesis, Institute of Nuclear Physics, Krakow, 1986, DESY-F31-86-02.
[17] R. Aaij *et al.* (LHCb Collaboration), J. High Energy Phys. 05 (2013) 159.
[18] C. Bobeth, G. Hiller, and D. van Dyk, J. High Energy Phys. 07 (2010) 098.
[19] R. Aaij *et al.* (LHCb Collaboration), Phys. Lett. B **708**, 241 (2012); R. Aaij *et al.* (LHCb Collaboration), Phys. Rev. Lett. **110**, 182001 (2013).
[20] R. Aaij *et al.* (LHCb Collaboration), Eur. Phys. J. C **72**, 2118 (2012).
[21] R. Aaij *et al.* (LHCb Collaboration), Nucl. Phys. **B874**, 663 (2013).

R. Aaij,[41] B. Adeva,[37] M. Adinolfi,[46] A. Affolder,[52] Z. Ajaltouni,[5] S. Akar,[6] J. Albrecht,[9] F. Alessio,[38] M. Alexander,[51] S. Ali,[41] G. Alkhazov,[30] P. Alvarez Cartelle,[37] A. A. Alves Jr.,[25,38] S. Amato,[2] S. Amerio,[22] Y. Amhis,[7] L. An,[3] L. Anderlini,[17,a] J. Anderson,[40] R. Andreassen,[57] M. Andreotti,[16,b] J. E. Andrews,[58] R. B. Appleby,[54]

O. Aquines Gutierrez,[10] F. Archilli,[38] A. Artamonov,[35] M. Artuso,[59] E. Aslanides,[6] G. Auriemma,[25,c] M. Baalouch,[5] S. Bachmann,[11] J. J. Back,[48] A. Badalov,[36] V. Balagura,[31] W. Baldini,[16] R. J. Barlow,[54] C. Barschel,[38] S. Barsuk,[7] W. Barter,[47] V. Batozskaya,[28] V. Battista,[39] A. Bay,[39] L. Beaucourt,[4] J. Beddow,[51] F. Bedeschi,[23] I. Bediaga,[1] S. Belogurov,[31] K. Belous,[35] I. Belyaev,[31] E. Ben-Haim,[8] G. Bencivenni,[18] S. Benson,[38] J. Benton,[46] A. Berezhnoy,[32] R. Bernet,[40] M.-O. Bettler,[47] M. van Beuzekom,[41] A. Bien,[11] S. Bifani,[45] T. Bird,[54] A. Bizzeti,[17,d] P. M. Bjørnstad,[54] T. Blake,[48] F. Blanc,[39] J. Blouw,[10] S. Blusk,[59] V. Bocci,[25] A. Bondar,[34] N. Bondar,[30,38] W. Bonivento,[15,38] S. Borghi,[54] A. Borgia,[59] M. Borsato,[7] T. J. V. Bowcock,[52] E. Bowen,[40] C. Bozzi,[16] T. Brambach,[9] J. van den Brand,[42] J. Bressieux,[39] D. Brett,[54] M. Britsch,[10] T. Britton,[59] J. Brodzicka,[54] N. H. Brook,[46] H. Brown,[52] A. Bursche,[40] G. Busetto,[22,e] J. Buytaert,[38] S. Cadeddu,[15] R. Calabrese,[16,b] M. Calvi,[20,f] M. Calvo Gomez,[36,g] P. Campana,[18,38] D. Campora Perez,[38] A. Carbone,[14,h] G. Carboni,[24,i] R. Cardinale,[19,38,j] A. Cardini,[15] L. Carson,[50] K. Carvalho Akiba,[2] G. Casse,[52] L. Cassina,[20] L. Castillo Garcia,[38] M. Cattaneo,[38] C. Cauet,[9] R. Cenci,[58] M. Charles,[8] P. Charpentier,[38] S. Chen,[54] S.-F. Cheung,[55] N. Chiapolini,[40] M. Chrzaszcz,[40,26] K. Ciba,[38] X. Cid Vidal,[38] G. Ciezarek,[53] P. E. L. Clarke,[50] M. Clemencic,[38] H. V. Cliff,[47] J. Closier,[38] V. Coco,[38] J. Cogan,[6] E. Cogneras,[5] P. Collins,[38] A. Comerma-Montells,[11] A. Contu,[15] A. Cook,[46] M. Coombes,[46] S. Coquereau,[8] G. Corti,[38] M. Corvo,[16,b] I. Counts,[56] B. Couturier,[38] G. A. Cowan,[50] D. C. Craik,[48] M. Cruz Torres,[60] S. Cunliffe,[53] R. Currie,[50] C. D'Ambrosio,[38] J. Dalseno,[46] P. David,[8] P. N. Y. David,[41] A. Davis,[57] K. De Bruyn,[41] S. De Capua,[54] M. De Cian,[11] J. M. De Miranda,[1] L. De Paula,[2] W. De Silva,[57] P. De Simone,[18] D. Decamp,[4] M. Deckenhoff,[9] L. Del Buono,[8] N. Déléage,[4] D. Derkach,[55] O. Deschamps,[5] F. Dettori,[38] A. Di Canto,[38] H. Dijkstra,[38] S. Donleavy,[52] F. Dordei,[11] M. Dorigo,[39] A. Dosil Suárez,[37] D. Dossett,[48] A. Dovbnya,[43] K. Dreimanis,[52] G. Dujany,[54] F. Dupertuis,[39] P. Durante,[38] R. Dzhelyadin,[35] A. Dziurda,[26] A. Dzyuba,[30] S. Easo,[49,38] U. Egede,[53] V. Egorychev,[31] S. Eidelman,[34] S. Eisenhardt,[50] U. Eitschberger,[9] R. Ekelhof,[9] L. Eklund,[51,38] I. El Rifai,[5] C. Elsasser,[40] S. Ely,[59] S. Esen,[11] H.-M. Evans,[47] T. Evans,[55] A. Falabella,[14] C. Färber,[11] C. Farinelli,[41] N. Farley,[45] S. Farry,[52] R. F. Fay,[52] D. Ferguson,[50] V. Fernandez Albor,[37] F. Ferreira Rodrigues,[1] M. Ferro-Luzzi,[38] S. Filippov,[33] M. Fiore,[16,b] M. Fiorini,[16,b] M. Firlej,[27] C. Fitzpatrick,[38] T. Fiutowski,[27] M. Fontana,[10] F. Fontanelli,[19,j] R. Forty,[38] O. Francisco,[2] M. Frank,[38] C. Frei,[38] M. Frosini,[17,38,a] J. Fu,[21,38] E. Furfaro,[24,i] A. Gallas Torreira,[37] D. Galli,[14,h] S. Gallorini,[22] S. Gambetta,[19,j] M. Gandelman,[2] P. Gandini,[59] Y. Gao,[3] J. García Pardiñas,[37] J. Garofoli,[59] J. Garra Tico,[47] L. Garrido,[36] C. Gaspar,[38] R. Gauld,[55] L. Gavardi,[9] G. Gavrilov,[30] E. Gersabeck,[11] M. Gersabeck,[54] T. Gershon,[48] P. Ghez,[4] A. Gianelle,[22] S. Giani',[39] V. Gibson,[47] L. Giubega,[29] V. V. Gligorov,[38] C. Göbel,[60] D. Golubkov,[31] A. Golutvin,[53,31,38] A. Gomes,[1,k] H. Gordon,[38] C. Gotti,[20] M. Grabalosa Gándara,[5] R. Graciani Diaz,[36] L. A. Granado Cardoso,[38] E. Graugés,[36] G. Graziani,[17] A. Grecu,[29] E. Greening,[55] S. Gregson,[47] P. Griffith,[45] L. Grillo,[11] O. Grünberg,[62] B. Gui,[59] E. Gushchin,[33] Y. Guz,[35,38] T. Gys,[38] C. Hadjivasiliou,[59] G. Haefeli,[39] C. Haen,[38] S. C. Haines,[47] S. Hall,[53] B. Hamilton,[58] T. Hampson,[46] X. Han,[11] S. Hansmann-Menzemer,[11] N. Harnew,[55] S. T. Harnew,[46] J. Harrison,[54] J. He,[38] T. Head,[38] V. Heijne,[41] K. Hennessy,[52] P. Henrard,[5] L. Henry,[8] J. A. Hernando Morata,[37] E. van Herwijnen,[38] M. Heß,[62] A. Hicheur,[1] D. Hill,[55] M. Hoballah,[5] C. Hombach,[54] W. Hulsbergen,[41] P. Hunt,[55] N. Hussain,[55] D. Hutchcroft,[52] D. Hynds,[51] M. Idzik,[27] P. Ilten,[56] R. Jacobsson,[38] A. Jaeger,[11] J. Jalocha,[55] E. Jans,[41] P. Jaton,[39] A. Jawahery,[58] F. Jing,[3] M. John,[55] D. Johnson,[55] C. R. Jones,[47] C. Joram,[38] B. Jost,[38] N. Jurik,[59] M. Kaballo,[9] S. Kandybei,[43] W. Kanso,[6] M. Karacson,[38] T. M. Karbach,[38] S. Karodia,[51] M. Kelsey,[59] I. R. Kenyon,[45] T. Ketel,[42] B. Khanji,[20] C. Khurewathanakul,[39] S. Klaver,[54] K. Klimaszewski,[28] O. Kochebina,[7] M. Kolpin,[11] I. Komarov,[39] R. F. Koopman,[42] P. Koppenburg,[41,38] M. Korolev,[32] A. Kozlinskiy,[41] L. Kravchuk,[33] K. Kreplin,[11] M. Kreps,[48] G. Krocker,[11] P. Krokovny,[34] F. Kruse,[9] W. Kucewicz,[26,l] M. Kucharczyk,[20,26,38,f] V. Kudryavtsev,[34] K. Kurek,[28] T. Kvaratskheliya,[31] V. N. La Thi,[39] D. Lacarrere,[38] G. Lafferty,[54] A. Lai,[15] D. Lambert,[50] R. W. Lambert,[42] G. Lanfranchi,[18] C. Langenbruch,[48] B. Langhans,[38] T. Latham,[48] C. Lazzeroni,[45] R. Le Gac,[6] J. van Leerdam,[41] J.-P. Lees,[4] R. Lefèvre,[5] A. Leflat,[32] J. Lefrançois,[7] S. Leo,[23] O. Leroy,[6] T. Lesiak,[26] B. Leverington,[11] Y. Li,[3] M. Liles,[52] R. Lindner,[38] C. Linn,[38] F. Lionetto,[40] B. Liu,[15] G. Liu,[38] S. Lohn,[38] I. Longstaff,[51] J. H. Lopes,[2] N. Lopez-March,[39] P. Lowdon,[40] H. Lu,[3] D. Lucchesi,[22,e] H. Luo,[50] A. Lupato,[22] E. Luppi,[16,b] O. Lupton,[55] F. Machefert,[7] I. V. Machikhiliyan,[31] F. Maciuc,[29] O. Maev,[30] S. Malde,[55] G. Manca,[15,m] G. Mancinelli,[6] J. Maratas,[5] J. F. Marchand,[4] U. Marconi,[14] C. Marin Benito,[36] P. Marino,[23,n] R. Märki,[39] J. Marks,[11] G. Martellotti,[25] A. Martens,[8] A. Martín Sánchez,[7] M. Martinelli,[41] D. Martinez Santos,[42] F. Martinez Vidal,[64] D. Martins Tostes,[2] A. Massafferri,[1] R. Matev,[38] Z. Mathe,[38] C. Matteuzzi,[20] A. Mazurov,[16,b] M. McCann,[53] J. McCarthy,[45] A. McNab,[54] R. McNulty,[12] B. McSkelly,[52] B. Meadows,[57] F. Meier,[9] M. Meissner,[11] M. Merk,[41] D. A. Milanes,[8] M.-N. Minard,[4] N. Moggi,[14] J. Molina Rodriguez,[60] S. Monteil,[5] M. Morandin,[22] P. Morawski,[27] A. Mordà,[6] M. J. Morello,[23,n] J. Moron,[27] A.-B. Morris,[50] R. Mountain,[59] F. Muheim,[50]

K. Müller,[40] M. Mussini,[14] B. Muster,[39] P. Naik,[46] T. Nakada,[39] R. Nandakumar,[49] I. Nasteva,[2] M. Needham,[50] N. Neri,[21] S. Neubert,[38] N. Neufeld,[38] M. Neuner,[11] A. D. Nguyen,[39] T. D. Nguyen,[39] C. Nguyen-Mau,[39,o] M. Nicol,[7] V. Niess,[5] R. Niet,[9] N. Nikitin,[32] T. Nikodem,[11] A. Novoselov,[35] D. P. O'Hanlon,[48] A. Oblakowska-Mucha,[27] V. Obraztsov,[35] S. Oggero,[41] S. Ogilvy,[51] O. Okhrimenko,[44] R. Oldeman,[15,m] G. Onderwater,[65] M. Orlandea,[29] J. M. Otalora Goicochea,[2] P. Owen,[53] A. Oyanguren,[64] B. K. Pal,[59] A. Palano,[13,p] F. Palombo,[21,q] M. Palutan,[18] J. Panman,[38] A. Papanestis,[49,38] M. Pappagallo,[51] C. Parkes,[54] C. J. Parkinson,[9,45] G. Passaleva,[17] G. D. Patel,[52] M. Patel,[53] C. Patrignani,[19,j] A. Pazos Alvarez,[37] A. Pearce,[54] A. Pellegrino,[41] M. Pepe Altarelli,[38] S. Perazzini,[14,h] E. Perez Trigo,[37] P. Perret,[5] M. Perrin-Terrin,[6] L. Pescatore,[45] E. Pesen,[66] K. Petridis,[53] A. Petrolini,[19,j] E. Picatoste Olloqui,[36] B. Pietrzyk,[4] T. Pilař,[48] D. Pinci,[25] A. Pistone,[19] S. Playfer,[50] M. Plo Casasus,[37] F. Polci,[8] A. Poluektov,[48,34] E. Polycarpo,[2] A. Popov,[35] D. Popov,[10] B. Popovici,[29] C. Potterat,[2] E. Price,[46] J. Prisciandaro,[39] A. Pritchard,[52] C. Prouve,[46] V. Pugatch,[44] A. Puig Navarro,[39] G. Punzi,[23,r] W. Qian,[4] B. Rachwal,[26] J. H. Rademacker,[46] B. Rakotomiaramanana,[39] M. Rama,[18] M. S. Rangel,[2] I. Raniuk,[43] N. Rauschmayr,[38] G. Raven,[42] S. Reichert,[54] M. M. Reid,[48] A. C. dos Reis,[1] S. Ricciardi,[49] S. Richards,[46] M. Rihl,[38] K. Rinnert,[52] V. Rives Molina,[36] D. A. Roa Romero,[5] P. Robbe,[7] A. B. Rodrigues,[1] E. Rodrigues,[54] P. Rodriguez Perez,[54] S. Roiser,[38] V. Romanovsky,[35] A. Romero Vidal,[37] M. Rotondo,[22] J. Rouvinet,[39] T. Ruf,[38] F. Ruffini,[23] H. Ruiz,[36] P. Ruiz Valls,[64] J. J. Saborido Silva,[37] N. Sagidova,[30] P. Sail,[51] B. Saitta,[15,m] V. Salustino Guimaraes,[2] C. Sanchez Mayordomo,[64] B. Sanmartin Sedes,[37] R. Santacesaria,[25] C. Santamarina Rios,[37] E. Santovetti,[24,i] A. Sarti,[18,s] C. Satriano,[25,c] A. Satta,[24] D. M. Saunders,[46] M. Savrie,[16,b] D. Savrina,[31,32] M. Schiller,[42] H. Schindler,[38] M. Schlupp,[9] M. Schmelling,[10] B. Schmidt,[38] O. Schneider,[39] A. Schopper,[38] M.-H. Schune,[7] R. Schwemmer,[38] B. Sciascia,[18] A. Sciubba,[25] M. Seco,[37] A. Semennikov,[31] I. Sepp,[53] N. Serra,[40] J. Serrano,[6] L. Sestini,[22] P. Seyfert,[11] M. Shapkin,[35] I. Shapoval,[16,43,b] Y. Shcheglov,[30] T. Shears,[52] L. Shekhtman,[34] V. Shevchenko,[63] A. Shires,[9] R. Silva Coutinho,[48] G. Simi,[22] M. Sirendi,[47] N. Skidmore,[46] T. Skwarnicki,[59] N. A. Smith,[52] E. Smith,[55,49] E. Smith,[53] J. Smith,[47] M. Smith,[54] H. Snoek,[41] M. D. Sokoloff,[57] F. J. P. Soler,[51] F. Soomro,[39] D. Souza,[46] B. Souza De Paula,[2] B. Spaan,[9] A. Sparkes,[50] P. Spradlin,[51] S. Sridharan,[38] F. Stagni,[38] M. Stahl,[11] S. Stahl,[11] O. Steinkamp,[40] O. Stenyakin,[35] S. Stevenson,[55] S. Stoica,[29] S. Stone,[59] B. Storaci,[40] S. Stracka,[23,38] M. Straticiuc,[29] U. Straumann,[40] R. Stroili,[22] V. K. Subbiah,[38] L. Sun,[57] W. Sutcliffe,[53] K. Swientek,[27] S. Swientek,[9] V. Syropoulos,[42] M. Szczekowski,[28] P. Szczypka,[39,38] D. Szilard,[2] T. Szumlak,[27] S. T'Jampens,[4] M. Teklishyn,[7] G. Tellarini,[16,b] F. Teubert,[38] C. Thomas,[55] E. Thomas,[38] J. van Tilburg,[41] V. Tisserand,[4] M. Tobin,[39] S. Tolk,[42] L. Tomassetti,[16,b] D. Tonelli,[38] S. Topp-Joergensen,[55] N. Torr,[55] E. Tournefier,[4] S. Tourneur,[39] M. T. Tran,[39] M. Tresch,[40] A. Tsaregorodtsev,[6] P. Tsopelas,[41] N. Tuning,[41] M. Ubeda Garcia,[38] A. Ukleja,[28] A. Ustyuzhanin,[63] U. Uwer,[11] V. Vagnoni,[14] G. Valenti,[14] A. Vallier,[7] R. Vazquez Gomez,[18] P. Vazquez Regueiro,[37] C. Vázquez Sierra,[37] S. Vecchi,[16] J. J. Velthuis,[46] M. Veltri,[17,t] G. Veneziano,[39] M. Vesterinen,[11] B. Viaud,[7] D. Vieira,[2] M. Vieites Diaz,[37] X. Vilasis-Cardona,[36,g] A. Vollhardt,[40] D. Volyanskyy,[10] D. Voong,[46] A. Vorobyev,[30] V. Vorobyev,[34] C. Voß,[62] H. Voss,[10] J. A. de Vries,[41] R. Waldi,[62] C. Wallace,[48] R. Wallace,[12] J. Walsh,[23] S. Wandernoth,[11] J. Wang,[59] D. R. Ward,[47] N. K. Watson,[45] D. Websdale,[53] M. Whitehead,[48] J. Wicht,[38] D. Wiedner,[11] G. Wilkinson,[55] M. P. Williams,[45] M. Williams,[56] F. F. Wilson,[49] J. Wimberley,[58] J. Wishahi,[9] W. Wislicki,[28] M. Witek,[26] G. Wormser,[7] S. A. Wotton,[47] S. Wright,[47] S. Wu,[3] K. Wyllie,[38] Y. Xie,[61] Z. Xing,[59] Z. Xu,[39] Z. Yang,[3] X. Yuan,[3] O. Yushchenko,[35] M. Zangoli,[14] M. Zavertyaev,[10,u] L. Zhang,[59] W. C. Zhang,[12] Y. Zhang,[3] A. Zhelezov,[11] A. Zhokhov,[31] L. Zhong[3] and A. Zvyagin[38]

(LHCb Collaboration)

[1]*Centro Brasileiro de Pesquisas Físicas (CBPF), Rio de Janeiro, Brazil*
[2]*Universidade Federal do Rio de Janeiro (UFRJ), Rio de Janeiro, Brazil*
[3]*Center for High Energy Physics, Tsinghua University, Beijing, China*
[4]*LAPP, Université de Savoie, CNRS/IN2P3, Annecy-Le-Vieux, France*
[5]*Clermont Université, Université Blaise Pascal, CNRS/IN2P3, LPC, Clermont-Ferrand, France*
[6]*CPPM, Aix-Marseille Université, CNRS/IN2P3, Marseille, France*
[7]*LAL, Université Paris-Sud, CNRS/IN2P3, Orsay, France*
[8]*LPNHE, Université Pierre et Marie Curie, Université Paris Diderot, CNRS/IN2P3, Paris, France*
[9]*Fakultät Physik, Technische Universität Dortmund, Dortmund, Germany*
[10]*Max-Planck-Institut für Kernphysik (MPIK), Heidelberg, Germany*
[11]*Physikalisches Institut, Ruprecht-Karls-Universität Heidelberg, Heidelberg, Germany*
[12]*School of Physics, University College Dublin, Dublin, Ireland*
[13]*Sezione INFN di Bari, Bari, Italy*

[14]Sezione INFN di Bologna, Bologna, Italy
[15]Sezione INFN di Cagliari, Cagliari, Italy
[16]Sezione INFN di Ferrara, Ferrara, Italy
[17]Sezione INFN di Firenze, Firenze, Italy
[18]Laboratori Nazionali dell'INFN di Frascati, Frascati, Italy
[19]Sezione INFN di Genova, Genova, Italy
[20]Sezione INFN di Milano Bicocca, Milano, Italy
[21]Sezione INFN di Milano, Milano, Italy
[22]Sezione INFN di Padova, Padova, Italy
[23]Sezione INFN di Pisa, Pisa, Italy
[24]Sezione INFN di Roma Tor Vergata, Roma, Italy
[25]Sezione INFN di Roma La Sapienza, Roma, Italy
[26]Henryk Niewodniczanski Institute of Nuclear Physics Polish Academy of Sciences, Kraków, Poland
[27]Faculty of Physics and Applied Computer Science, AGH - University of Science and Technology, Kraków, Poland
[28]National Center for Nuclear Research (NCBJ), Warsaw, Poland
[29]Horia Hulubei National Institute of Physics and Nuclear Engineering, Bucharest-Magurele, Romania
[30]Petersburg Nuclear Physics Institute (PNPI), Gatchina, Russia
[31]Institute of Theoretical and Experimental Physics (ITEP), Moscow, Russia
[32]Institute of Nuclear Physics, Moscow State University (SINP MSU), Moscow, Russia
[33]Institute for Nuclear Research of the Russian Academy of Sciences (INR RAN), Moscow, Russia
[34]Budker Institute of Nuclear Physics (SB RAS) and Novosibirsk State University, Novosibirsk, Russia
[35]Institute for High Energy Physics (IHEP), Protvino, Russia
[36]Universitat de Barcelona, Barcelona, Spain
[37]Universidad de Santiago de Compostela, Santiago de Compostela, Spain
[38]European Organization for Nuclear Research (CERN), Geneva, Switzerland
[39]Ecole Polytechnique Fédérale de Lausanne (EPFL), Lausanne, Switzerland
[40]Physik-Institut, Universität Zürich, Zürich, Switzerland
[41]Nikhef National Institute for Subatomic Physics, Amsterdam, The Netherlands
[42]Nikhef National Institute for Subatomic Physics and VU University Amsterdam, Amsterdam, The Netherlands
[43]NSC Kharkiv Institute of Physics and Technology (NSC KIPT), Kharkiv, Ukraine
[44]Institute for Nuclear Research of the National Academy of Sciences (KINR), Kyiv, Ukraine
[45]University of Birmingham, Birmingham, United Kingdom
[46]H.H. Wills Physics Laboratory, University of Bristol, Bristol, United Kingdom
[47]Cavendish Laboratory, University of Cambridge, Cambridge, United Kingdom
[48]Department of Physics, University of Warwick, Coventry, United Kingdom
[49]STFC Rutherford Appleton Laboratory, Didcot, United Kingdom
[50]School of Physics and Astronomy, University of Edinburgh, Edinburgh, United Kingdom
[51]School of Physics and Astronomy, University of Glasgow, Glasgow, United Kingdom
[52]Oliver Lodge Laboratory, University of Liverpool, Liverpool, United Kingdom
[53]Imperial College London, London, United Kingdom
[54]School of Physics and Astronomy, University of Manchester, Manchester, United Kingdom
[55]Department of Physics, University of Oxford, Oxford, United Kingdom
[56]Massachusetts Institute of Technology, Cambridge, Massachusetts, USA
[57]University of Cincinnati, Cincinnati, Ohio, USA
[58]University of Maryland, College Park, Maryland, USA
[59]Syracuse University, Syracuse, New York, USA
[60]Pontifícia Universidade Católica do Rio de Janeiro (PUC-Rio), Rio de Janeiro, Brazil
(associated with Universidade Federal do Rio de Janeiro (UFRJ), Rio de Janeiro, Brazil)
[61]Institute of Particle Physics, Central China Normal University, Wuhan, Hubei, China
(associated with Center for High Energy Physics, Tsinghua University, Beijing, China)
[62]Institut für Physik, Universität Rostock, Rostock, Germany
(associated with Physikalisches Institut, Ruprecht-Karls-Universität Heidelberg, Heidelberg, Germany)
[63]National Research Centre Kurchatov Institute, Moscow, Russia
(associated with Institute of Theoretical and Experimental Physics (ITEP), Moscow, Russia)
[64]Instituto de Fisica Corpuscular (IFIC), Universitat de Valencia-CSIC, Valencia, Spain
(associated with Universitat de Barcelona, Barcelona, Spain)
[65]KVI - University of Groningen, Groningen, The Netherlands
(associated with Nikhef National Institute for Subatomic Physics, Amsterdam, The Netherlands)
[66]Celal Bayar University, Manisa, Turkey
(associated with European Organization for Nuclear Research (CERN), Geneva, Switzerland)

[a]Also at Università di Firenze, Firenze, Italy.
[b]Also at Università di Ferrara, Ferrara, Italy.
[c]Also at Università della Basilicata, Potenza, Italy.
[d]Also at Università di Modena e Reggio Emilia, Modena, Italy.
[e]Also at Università di Padova, Padova, Italy.
[f]Also at Università di Milano Bicocca, Milano, Italy.
[g]Also at LIFAELS, La Salle, Universitat Ramon Llull, Barcelona, Spain.
[h]Also at Università di Bologna, Bologna, Italy.
[i]Also at Università di Roma Tor Vergata, Roma, Italy.
[j]Also at Università di Genova, Genova, Italy.
[k]Also at Universidade Federal do Triângulo Mineiro (UFTM), Uberaba-MG, Brazil.
[l]Also at AGH - University of Science and Technology, Faculty of Computer Science, Electronics and Telecommunications, Kraków, Poland.
[m]Also at Università di Cagliari, Cagliari, Italy.
[n]Also at Scuola Normale Superiore, Pisa, Italy.
[o]Also at Hanoi University of Science, Hanoi, Vietnam.
[p]Also at Università di Bari, Bari, Italy.
[q]Also at Università degli Studi di Milano, Milano, Italy.
[r]Also at Università di Pisa, Pisa, Italy.
[s]Also at Università di Roma La Sapienza, Roma, Italy.
[t]Also at Università di Urbino, Urbino, Italy.
[u]Also at P.N. Lebedev Physical Institute, Russian Academy of Science (LPI RAS), Moscow, Russia.